Sustainable, low Ni-containing Mg-doped layered oxides as cathodes for sodium-ion batteries

Table S1: Comparison of previously reported electrochemical performances of related cathodes with our best material.

	Low rate / mA h g^{-1} (C rate) voltage limits /V	High rate / mA h g^{-1} (C rate) voltage limits /V	Reference
$Na_{0.57}[Li_{0.1}(Fe_{0.5}Mn_{0.5})_{0.9}]O_2$	200 (C/10) 1.5-4.3	60 (5C) 1.5-4.3	[1]
$Na_{0.5}[Ni_{0.23}Fe_{0.13}Mn_{0.63}]O_2$	200 (C/10) 1.5-4.6	60 (5C) 1.5-4.6	[2]
$Na_{2/3}Fe_{1/2}Mn_{1/2}O_2$	160 (C/10) 1.5-4.25	N/A	[3]
F-doped $Na_{0.67}[Mg_{0.28}Mn_{0.72}]O_2$	140 (C/10) 1.5-4.4	~50 (3C) 1.5-4.4	[4]
$Na_{2/3}Mn_{0.8}Fe_{0.1}Mg_{0.1}O_2$	168 (C/10) 1.5-4.2	80 (5C) 1.5-4.2	[5]
$Na_{0.67}Fe_{0.425}Mn_{0.425}Mg_{0.15}O_2$	146.6 (C/10) 1.5-4.2	58.4 (2C) 1.5-4.2	[6]
$Na_{0.8}Mn_{0.5}Fe_{0.5}O_2$	180 (C/5) 1.5-4.2 V	35 (4C) 1.5-4.2	[7]
$Na_{0.67}Fe_{0.4}Mn_{0.5}Mg_{0.1}O_2$	127.5 (C/2) 2.0-4.3	ca. 50, (5C) 2.0-4.3	[8]
$Na_{0.67}Fe_{0.5}Mn_{0.46}Mg_{0.04}O_2$	182.04 (C/5) 1.5-4.2	ca. 20, (5C) 1.5-4.2	[9]
$Na_{0.67}Mg_{0.05}Ni_{0.05}Mn_{0.9}O_2$	201.4 (C/10) 1.5-4.5	102 (5C) 1.5-4.5	This work

N/A: Not available data

1 S. G. Lim, M.-S. Kwon, T. Kim, H. Kim, S. Lee, J. Lim, H. Kim, K. T. Lee, *ACS Appl. Mater. Interfaces*, 2022, **14**, 33120.

2 I. Hasa, D. Buchholz, S. Passerini, B. Scrosati, J. Hassoun, *Adv. Energy Mater.*, 2014, **4**, 1400083.

3 J. S. Thorne, R. A. Dunlap, M. N. Obrovac, *J. Electrochem. Soc*. 2013, **160**, A361.

4 F. P. Nkosi, K. Raju, N. Palaniyandy, M. V. Reddy, C. Billing, K. I. Ozoemena, *J. Electrochem. Soc.*, 2017,**164**, A3362.

5 Y. Li, Z.-Y. Li, K. Sun, Y.-T. Liu, D.-F. Chen, S.-B. Han, L.-F. He, M.-J. Li, X.-L. Liu, M.-M. Wu, *Ionics*, 2020, **26**, 735.

6 D. Zhou, W. Huang, X. Lv, F. Zhao, *J. Power Sources*, 2019, **421**, 147.

7 J. Yang, A. E. Maughan, G. Teeter, B. J. Tremolet de Villers, S.-M. Bak, S.-D. Han, *ChemSusChem*, 2020, **13**, 5972.

8 J. Wang, J. Luo, B. Zhao, G. Zhao, B. Huang, *Ionics*, 2023, **29**, 833.

9 D. Zhou, C. Zeng, D. Ling, T. Wang, Z. Gao, J. Li, L. Tian, Y. Wang, W. Huang, *J. Alloys Compd.* 2023, **931**, 167567.

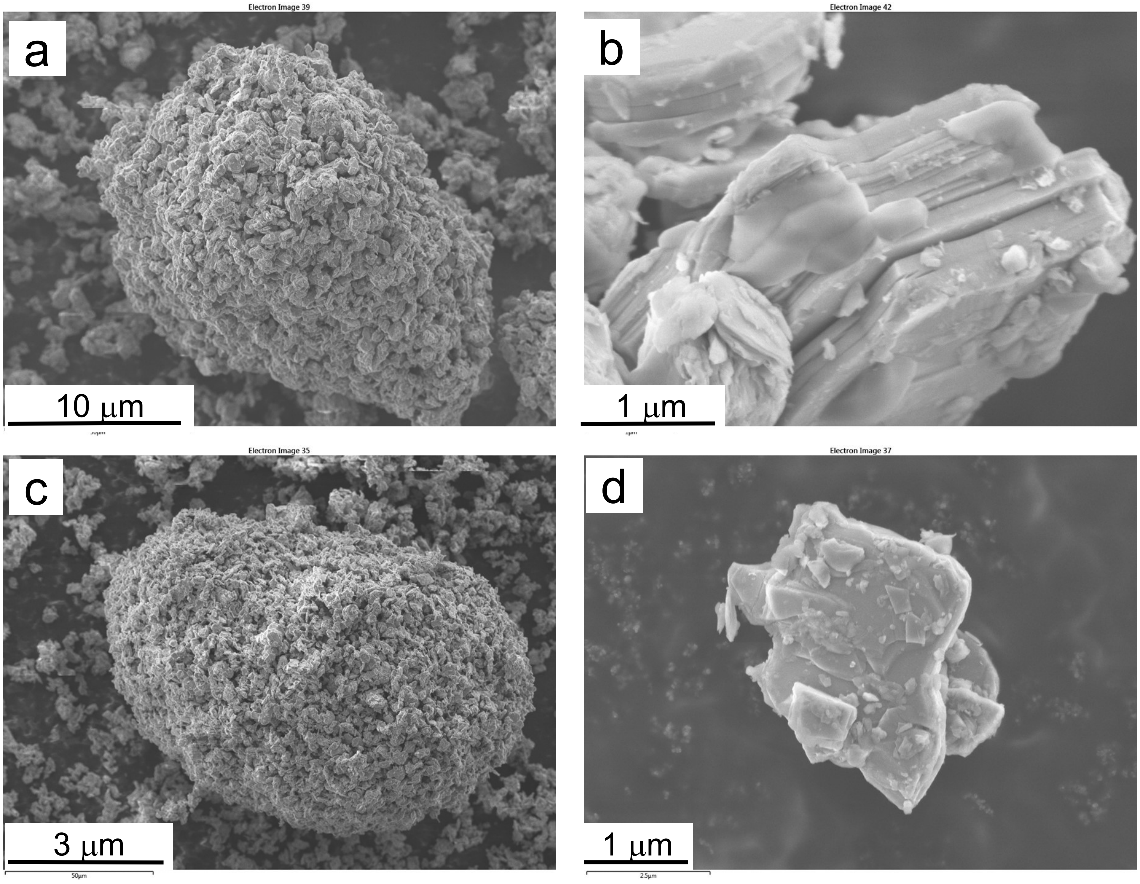

Figure S1. FE-SEM micrographs of a, b) F0N05 and c, d) F1N15 at two different magnifications.

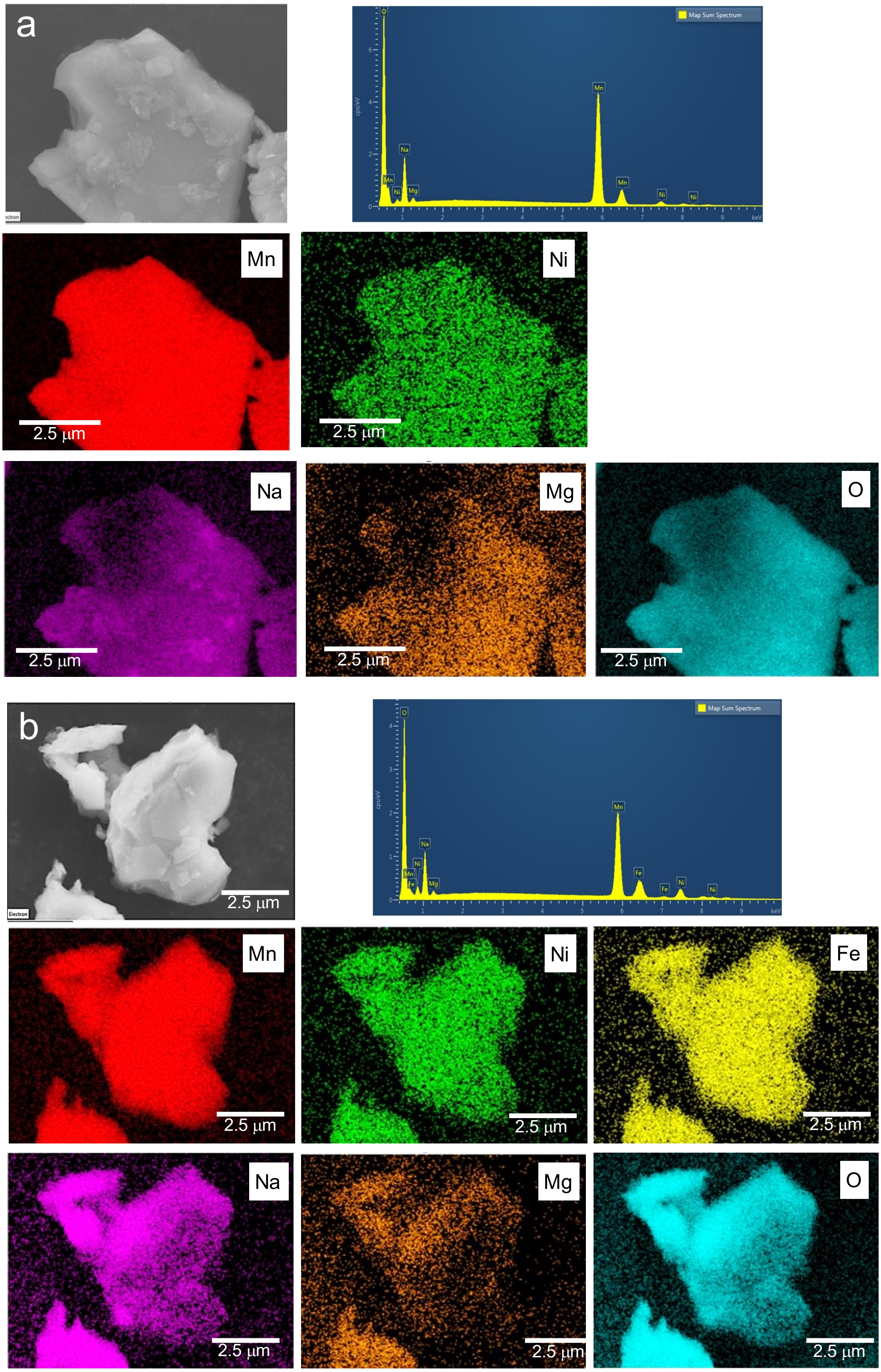

Figure S2: EDX spectrum and maps for elements, Na, Mg, Fe, Ni, Mn, and O for a) F0N05; b) and F1N15 samples

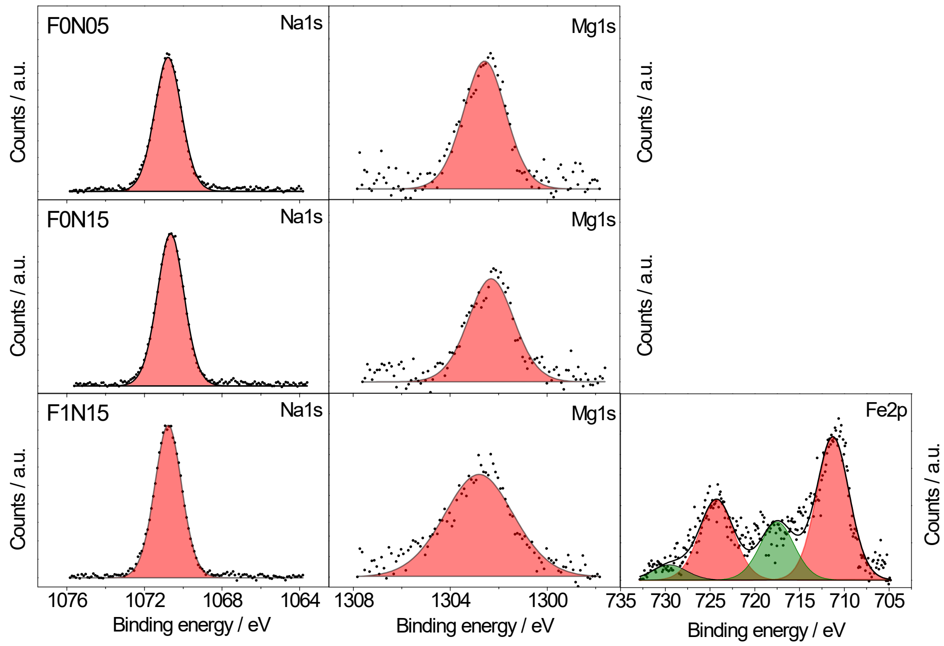

Figure S3: XPS sub-spectra recorded at the Na1s, Mg1s and Fe2p core levels of F0N05, F0N15 and F1N15 samples.

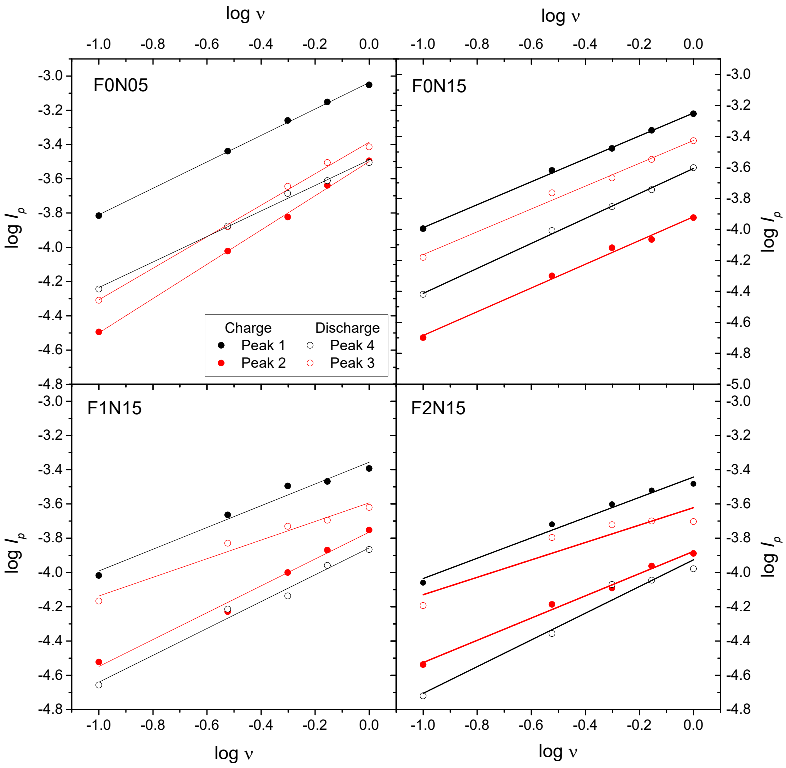

Figure S4: Linear fitting of the log I versus log *v* plots of the anodic and cathodic peaks, derived from the cyclic voltammograms recorded after one cycle at C/10 in Figure 5, for the studied samples.

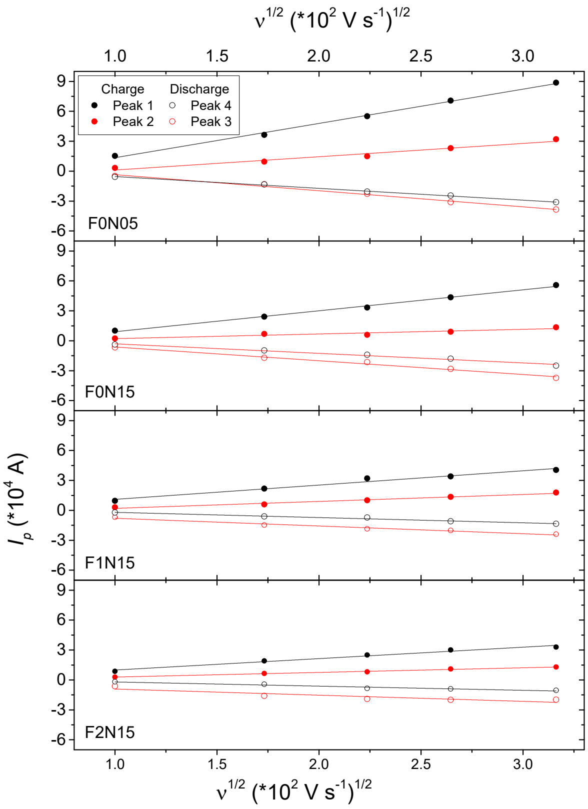

Figure S5: Plots of the peak current (I_p) versus the square root of the scan rate ($\nu^{1/2}$), derived from the cyclic voltammograms recorded after one cycle at C/10 in Figure 5, used for the calculation of the apparent diffusion coefficients based on the Randles-Sevcik equation.

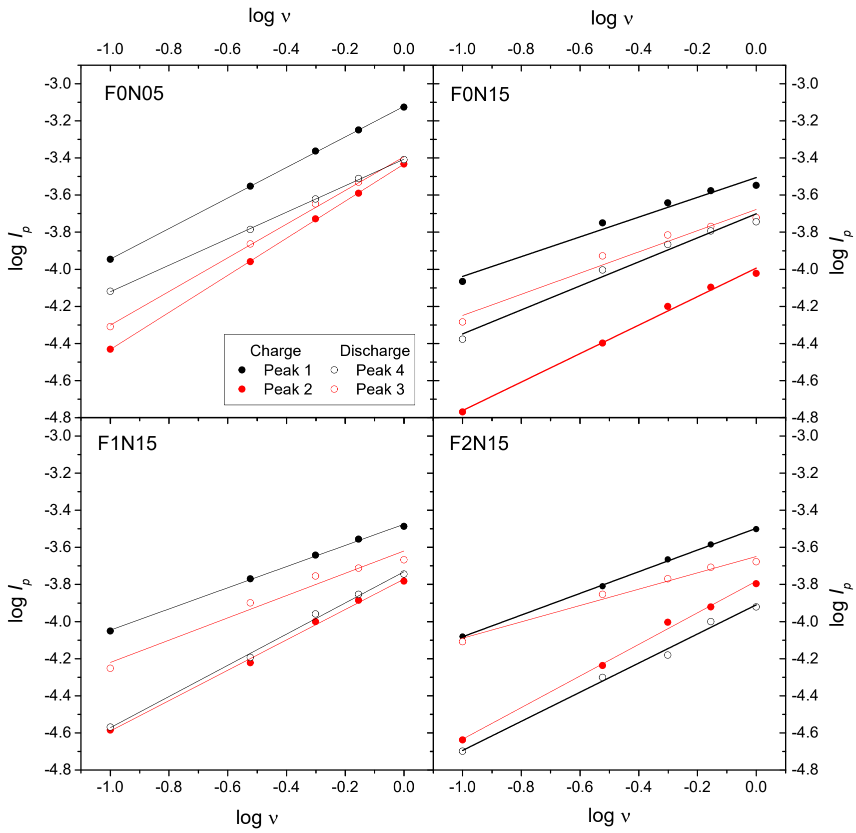

Figure S6: Linear fitting of the log I versus log *v* plots of the anodic and cathodic peaks, derived from the cyclic voltammograms recorded after the 100th cycle at 1C in Figure 9, for the studied samples.

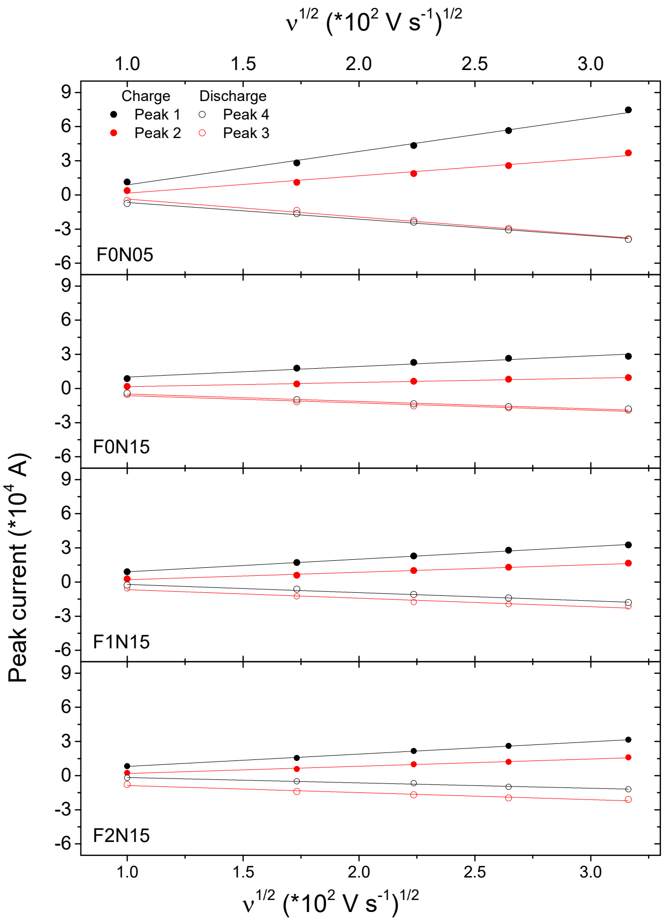

Figure S7: Plots of the peak current (I_p) versus the square root of the scan rate ($\nu^{1/2}$), derived from the cyclic voltammograms recorded after the 100th cycle at 1C in Figure 9, used for the calculation of the apparent diffusion coefficients based on the Randles-Sevcik equation.